Estimating total and remanent magnetization of geological sources: petrophysical measurements, borehole logging, and anomaly analysis

David A. Clark[1]

1. CSIRO Manufacturing, Superconducting Systems and Devices Group, & CSIRO Minerals

ABSTRACT

Assuming without evidence that magnetic sources are magnetized parallel to the geomagnetic field can seriously mislead interpretation and can result in drill holes missing their targets. I review methods that are available for estimating, directly or indirectly, the natural remanent magnetization (NRM) and total magnetization of magnetic sources, noting the strengths and weaknesses of each approach. Particular attention is paid to: magnetic property measurements of samples, and inference of magnetic properties from borehole magnetic measurements. I also discuss what information about magnetization of sources can be extracted from analysis of magnetic anomalies, based on assumptions about the sources or constraints from geological information or other geophysical methods.

INTRODUCTION

Magnetic anomalies are perturbations of the geomagnetic main field that are produced by magnetization contrasts within the Earth's lithosphere. Although the distribution of magnetization is heterogeneous over a wide range of scales, in many cases magnetic sources can be adequately represented by discrete bodies with effectively uniform magnetization, surrounded by a uniformly magnetized medium. These sources may represent distinct rock units, ore bodies, zones of alteration (metamorphic or hydrothermal), buried ferrous objects etc., depending on the geological environment and the scale of the anomalies.

The total magnetization **M** of a geological source is the vector sum of two contributions: induced magnetization and natural remanent magnetization (NRM):

$$\mathbf{M} = \mathbf{M}_{\mathrm{NRM}} + \mathbf{M}_{\mathrm{IND}} \tag{1}$$

where $\mathbf{M}_{\mathrm{IND}}$ is a function of the applied field **F** and $\mathbf{M}_{\mathrm{NRM}}$ is independent of **F**. Because the geomagnetic field is relatively weak, the induced magnetization is proportional to **F**, to a good approximation. In the general case, where the source is magnetically anisotropic

$$\mathbf{M} = \mathbf{M}_{\mathrm{NRM}} + \mathbf{KF} \tag{2}$$

where **K** is the magnetic susceptibility tensor. Equation (2) is a matrix equation, where $\mathbf{M}_{\mathrm{NRM}}$, $\mathbf{M}_{\mathrm{IND}}$ and **F** are column vectors and **K** is a 3 × 3 symmetric matrix with the susceptibility tensor components as its elements. If the susceptibility is isotropic, $\mathbf{K} = k\mathbf{I}$, where **I** is the identity matrix and k is the isotropic susceptibility. Note that in SI susceptibilities are dimensionless and magnetizations are conventionally expressed in A/m, so **F** in equations (2)-(3) must also be given in A/m. For example, if the geomagnetic field is given as B = 50,000 nT, then $F = 50{,}000\times10^{-9}/(4\pi\times10^{-7}) = 39.8$ A/m.

Clark (1997) has reviewed the susceptibility and remanence properties of magnetic minerals and the rocks that contain them. Figure 1 plots the susceptibility ranges generally observed for common rock types. Effects of hydrothermal alteration on susceptibilities of protoliths of various compositions in porphyry copper and IOCG mineralized systems have been reviewed by Clark (2014a).

A source with strong magnetization produces an internal field (the self-demagnetizing field) that perturbs the geomagnetic field significantly. The effect is to reduce the effective inducing field and, if the source is not equidimensional, to deflect the induced magnetization away from the inducing field direction. As a rule of thumb, self-demagnetization corrections are significant for susceptibilities above ~0.1 SI and are crucial for k > 0.5 SI.

Exact analytic corrections for self-demagnetization are only available for ellipsoidal sources with homogeneous properties. The resultant magnetization $\mathbf{M}'$ of an ellipsoid, in a uniform external applied field $\mathbf{F}_0$, with uniform *intrinsic* remanence $\mathbf{M}_{\mathrm{NRM}}$ and homogeneous, but anisotropic, *intrinsic* susceptibility **K**, corrected for self-demagnetization, is given by:

$$\mathbf{M}' = (\mathbf{I} + \mathbf{KN})^{-1}(\mathbf{M}_{\mathrm{NRM}} + \mathbf{KF}_0), \tag{3}$$

where **N** is the demagnetising tensor (Clark et al., 1986). **N** is a symmetric second order tensor, with unit trace if SI units are used. The eigenvectors $\mathbf{v}_i$ (i = 1,2,3) of the demagnetising tensor are parallel to the ellipsoid axes. The corresponding eigenvalues of **N** are the demagnetising factors N_1, N_2, N_3 along the ellipsoid axes. Clark et al. (1986) give expressions for the demagnetising factors of triaxial ellipsoids.

If the susceptibility is isotropic, the magnetization components with respect to these principal axes are:

$$M_i' = \frac{M_{NRM}^i + kF_i}{1 + kN_i}, \quad (i = 1,2,3). \tag{4}$$

Determining the intrinsic magnetic properties of strongly magnetic samples from laboratory measurements of their demagnetization-controlled properties requires inverting (3). In the most general case, for inequidimensional, anisotropic specimens, the demagnetization-corrected intrinsic properties are given by:

$$\mathbf{K} = (\mathbf{I} - \mathbf{K}'\mathbf{N})^{-1}\mathbf{K}'; \ \mathbf{M}_{NRM} = (\mathbf{I} + \mathbf{KN})\mathbf{M}'_{NRM}, \quad (5)$$

Emerson et al. (1985) give formulae for the exact demagnetising factors of useful limiting cases of ellipsoids (spheres, infinite circular and elliptic cylinders, infinite sheets, prolate spheroids, and oblate spheroids), as well as approximate demagnetising factors for prisms and cylinders.

The Koenigsberger ratio Q describes the relative strength of remanent and induced magnetizations, i.e.

$$Q = |\mathbf{M}_{NRM}|/|\mathbf{M}_{IND}|. \quad (6)$$

Q is a scalar parameter that is independent of the magnetization direction. Other useful parameters that characterise the importance of remanence are the angular differences θ and θ_{NRM} between the inducing field and, respectively, the resultant magnetization and the remanence, i.e.

$$\left.\begin{aligned} \theta &= \cos^{-1}(\hat{\mathbf{M}}.\hat{\mathbf{F}}) \\ \theta_{NRM} &= \cos^{-1}(\hat{\mathbf{M}}_{NRM}.\hat{\mathbf{F}}) \end{aligned}\right\}; \ 0° \le \theta \le \theta_{NRM} \le 180°, \quad (7)$$

where the hats indicate unit vectors. Clark (2014b) gives useful expressions for relationships between these angles and the Koenigsberger ratio. Figure 2 plots typical Q values for common lithologies.

Figure 3 illustrates a general principle that densities of broadly defined igneous and metamorphic rock types have a unimodal distribution and are fairly predictable. This is because the density reflects the relative proportions of the major minerals that are used to name the rock. On the other hand, susceptibilities of broadly defined rock types exhibit a bimodal distribution, because the susceptibility depends on the composition and abundance of accessory minerals, such as magnetite, that are ignored in classifying the lithology. The bimodal distribution reflects the presence of distinct paramagnetic and ferromagnetic subpopulation. Only the ferromagnetic subpopulation contains more than trace amounts of strongly magnetic oxide or sulfide minerals.

The dominant control on whether a rock unit belongs to the paramagnetic or ferromagnetic subpopulation is the oxidation state, which is generally inherited from the magmatic source region (for igneous rocks) or the protolith (for metamorphic rocks) (Puranen, 1989; Clark, 1997, 1999). A convenient measure of the oxidation state is the ratio of ferric iron to total iron in the rock. Although Figure 3 suggests that the susceptibility of a particular rock type is quite unpredictable, in practice susceptibility distributions within particular geological provinces tend to be much narrower and igneous rocks that belong to specific magmatic series have fairly predictable susceptibilities that vary systematically with bulk composition (e.g. silica content), hence with rock name. Furthermore, refined classification of rocks that includes varietal mineralogy can often predict whether a rock unit belongs to the paramagnetic or ferromagnetic category (Clark, 1997, 1999). For metamorphic rocks, the susceptibility is a function of the inherited oxidation state, bulk composition and metamorphic grade, which determines into which minerals (e.g. hydrous silicates versus oxides plus anhydrous silicates) ferric and ferrous iron can be partitioned.

Characterising the total and remanent magnetizations of sources is important for several reasons. Knowledge of total magnetization is often critical for accurate determination of source geometry and position. Knowledge of magnetic properties such as magnetization intensity and Koenigsberger ratio constrains the likely magnetic mineralogy (composition and grain size) of a source, which gives an indication of its geological nature. Determining the direction of a stable ancient remanence gives an indication of the age of magnetization, which provides useful information about the geological history of the source and its environs. Several methods exist for estimating the magnetic moment vector of a source, without any knowledge of its shape. This yields directions of the resultant magnetization (remanent plus induced) and gives an indication of the size of the source, when plausible magnetization intensities are assumed.

PETROPHYSICAL MEASUREMENTS

Sampling requirements

Reliable quantitative estimation of magnetization of a source (e.g. a rock unit, orebody, alteration zone, structural zone) from samples requires:

1. extensive sampling of a representative portion of the source (and its surroundings, if the environment is magnetic),
2. well-calibrated susceptibility and NRM measurements on standard samples (or with accurately determined corrections for non-standard samples),
3. correction of apparent susceptibility and remanence measurements for self-demagnetization effects, to obtain the corresponding intrinsic properties, for sample susceptibilities greater than ~0.1 SI,
4. careful analysis of measured remanence data to determine if measured sample NRMs are contaminated by spurious components, such as drilling-induced remanence, lightning effects, or isothermal components acquired since sampling (e.g. from logging with pencil magnets), to remove these spurious components by palaeomagnetic cleaning, and to decompose complex multi-component NRM into its constituent components (each of which records a separate geological event or geomagnetic environment),
5. rigorous statistical analysis to estimate bulk mean properties, with error estimates, that recognises the vector nature of magnetization and, if the samples are anisotropic, the tensor nature of susceptibility.

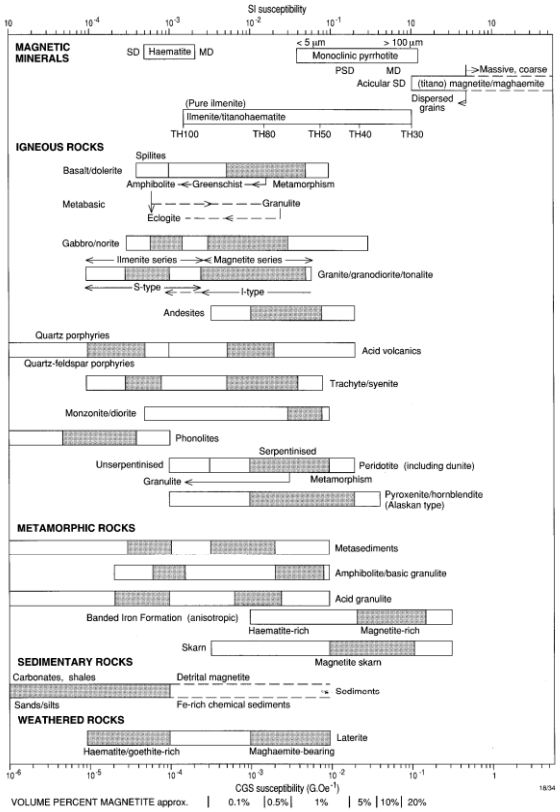

Figure 1. Range of magnetic susceptibilities for important magnetic minerals and major rock types (after Clark, 1997). Stippled portions of bars indicate common susceptibility ranges for various lithologies. Note the bimodal susceptibility distributions for many rock types.

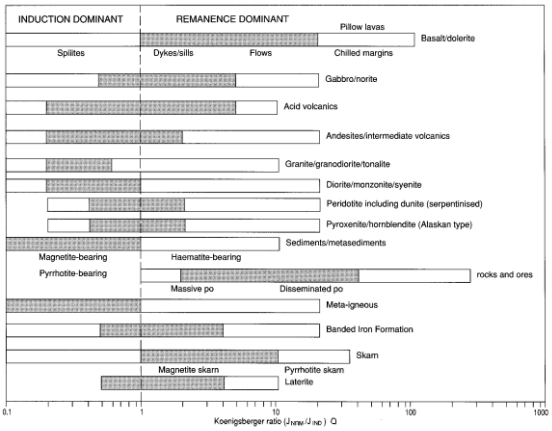

Figure 2. Observed and common (shaded) ranges of Koenigsberger ratios for important magnetic minerals and major rock types (after Clark, 1997).

Statistical analysis of susceptibility measurements

It can be seen from Figure 3 that, for each rock type, susceptibility distributions for each of the two distinct unimodal subpopulations is approximately symmetric when plotted on a logarithmic scale. Empirically, it is often found that the susceptibility distributions from individual rock units are approximately lognormal.

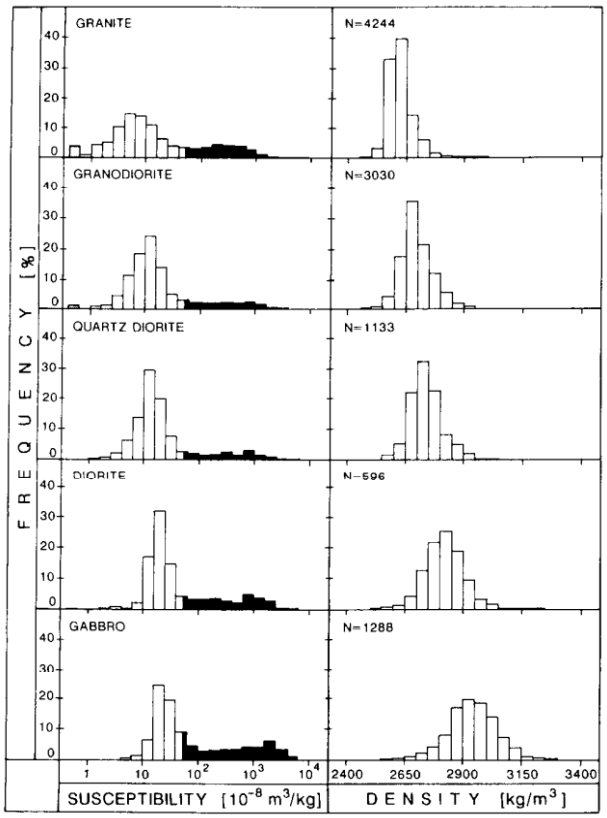

Figure 3. Histograms of SI mass susceptibility and density for plutonic rock types from Finland (after Puranen, 1989). Note the unimodal density distribution contrasting with the bimodal susceptibility distribution. The ferromagnetic subpopulation is shown as black. To convert mass susceptibility to SI volume susceptibility, multiply by the density in kg/m^3.

Although the susceptibilities within a rock unit may be highly variable over short distances, the measured magnetic anomaly reflects the bulk susceptibility, averaged over large volumes of rock. For the purposes of magnetic modelling, therefore, the bulk induced magnetization of a rock unit should be calculated from its estimated *arithmetic* mean susceptibility. Provided the unit has been adequately and representatively sampled, and there are no large scale trends in the susceptibility, the arithmetic mean of the susceptibility measurements is an unbiased estimator of the bulk average susceptibility of the unit, modelled as a homogeneous geometric body, irrespective of the underlying distribution of susceptibilities.

For a large number of samples the sample mean will have an approximately Gaussian distribution and the standard error of the mean can therefore be used to place confidence limits on the estimated bulk susceptibility. However, if the underlying distribution of susceptibilities is actually lognormal, then a more robust and precise estimate of the mean bulk susceptibility can be obtained by calculating the minimum variance unbiased estimator (Aitchison, 1955; Aitchison and Brown, 1963).

If the natural logarithms of susceptibilities drawn from the population have a Gaussian distribution with mean μ and variance σ^2, i.e. $ln(k) \sim N(\mu,\sigma^2)$, then the distribution of

susceptibilities is lognormal, $k \sim LN(\mu,\sigma^2)$. The median and geometric mean of the lognormal distribution are both equal to $\exp(\mu)$ and the geometric standard deviation factor is $\exp(\sigma)$. The arithmetic mean of the population is $\exp(\mu+\sigma^2/2)$ and its variance is $[\exp(\sigma^2) - 1]\ \exp(2\mu+\sigma^2)$. For a sample of n measurements, the minimum variance unbiased estimator of the arithmetic mean is given by:

$$\hat{k} = \exp(\hat{\mu})\psi_n(\hat{\sigma}^2/2), \tag{8}$$

where

$$\hat{\mu} = \frac{1}{n}\sum_{i=1}^{n}\ln(k_i), \tag{9}$$

is an estimator of the mean μ of the distribution of $\ln(k)$,

$$\hat{\sigma}^2 = \frac{1}{n-1}\sum_{i=1}^{n}[\ln(k_i) - \ln\hat{k}]^2, \tag{10}$$

is an estimator of the variance σ^2 of the distribution of $\ln(k)$, and

$$\begin{aligned}\psi_n(t) &= 1 + \frac{n-1}{n}t + \frac{(n-1)^3}{n^2 2!}\frac{t^2}{n+1} \\ &\quad + \frac{(n-1)^5}{n^3 3!}\frac{t^3}{(n+1)(n+3)} + ... \\ &\approx e^t\left[1 - \frac{t(t+1)}{n}t + \frac{t^2(3t^2+22t+21)}{6n^2}\right] + O\left(\frac{1}{n_3}\right).\end{aligned} \tag{11}$$

The minimum variance unbiased estimator of the variance of the estimated arithmetic mean is given by:

$$\mathrm{var}(\hat{k}) = \exp(2\hat{\mu})\left[\psi_n(2\hat{\sigma}^2) - \psi_n\left(\frac{n-2}{n-1}\hat{\sigma}^2\right)\right], \tag{12}$$

which can be used to calculate confidence intervals by assuming that the estimated means are normally distributed, to a good approximation (Owen and DeRouen, 1980).

It is quite common that samples from a relatively magnetic rock unit, with susceptibilities that generally belong to a lognormally distributed ferromagnetic population, occasionally have much lower susceptibilities in, for example, quartz veins or local patches of intense alteration. In this case the distribution may be modelled as a lognormal population with zeroes, which can be handled as a delta distribution for the purposes of estimation (Owen and DeRouen, 1980).

Paleomagnetic cleaning of measured NRMs

Measured NRMs of samples are often contaminated by palaeomagnetic noise. In this context, palaeomagnetic noise refers to components that are unrepresentative of the *in situ* remanence, such as isothermal remanence (IRM) components acquired through exposure to moderate to strong magnetic fields; drilling-induced remanence acquired in the magnetic field inside the core barrel, due to stress release during coring; chemical remanent magnetization (CRM) components associated with alteration of magnetic minerals in surface samples by weathering; or short term viscous remanence (VRM) components acquired post-collection in weak ambient fields, either by very "soft" large MD grains or by ultrafine single domain (SD) grains around the superparamagnetic (SPM)-stable SD transition. However long term VRM acquired in the geomagnetic field since the last geomagnetic reversal is representative of the bulk *in situ* magnetization and is not categorised here as noise, although it is an annoyance to palaeomagnetists (unless it is used for core orientation), who are mainly interested in ancient remanence components. Lightning strikes are common sources of IRM noise in outcrop and very near surface samples, particularly on hilltops and in areas with low erosion rates. Mining operations and logging with pencil magnets often contaminate measured NRMs.

The most common palaeomagnetic cleaning methods are alternating field (AF) demagnetization, which initially removes remanence carried by grains with low coercivity then, as it proceeds, progressively higher coercivities, and thermal demagnetization, which successively unblocks increasingly stable components of remanence. Low temperature demagnetization, accomplished by cooling specimens in liquid nitrogen and then rewarming to room temperature in zero magnetic field, is a useful pre-treatment for removing soft palaeomagnetic noise components, such as IRMs and drilling-induced remanence, carried by MD magnetite or hematite grains, while leaving more stable remanence components relatively unaffected.

Figure 4 illustrates the principle of palaeomagnetic cleaning of measured NRMs that are unrepresentative of the bulk *in situ* remanence, in order to estimate the true contribution of remanence to the magnetization of the sampled source. The measured NRM of the sample comprises three components: a stable ancient TRM, a VRM overprint acquired over the Brunhes chron, and an IRM noise component. If the stability spectra of three components do not overlap, appropriate stepwise demagnetization of the NRM allows the components to be separated cleanly. In that case, successive remanence vector end-points define three linear segments; the initial segment corresponds to the IRM, the intermediate segment represents the VRM, and the final segment, which heads directly towards the origin, corresponds to the TRM. Decomposition of the NRM vector into its three constituent components is then straightforward.

As can be seen in Figure 4, if the stability spectra of the different components overlap, the demagnetization paths are curved through the transition between linear segments, where two or more components are being demagnetized simultaneously. If overlap of stability spectra is not complete, as is generally the case, the directions of the remanence components can be determined by fitting least-squares best-fit lines to the linear segments from individual specimens (Kirschvink, 1980; Kent et al., 1983) or groups of specimens (Schmidt, 1982). If overlap of spectra precludes well-defined linear segments, other analysis methods such as Hoffman-Day plots (Hoffman and Day, 1978; Halls, 1979) or remagnetization circles (Halls, 1976; McFadden and McElhinny, 1988), with the caveats discussed by Schmidt (1985), can be used to extract the component directions. Once the directions associated with each component are determined, the contribution of each

component to the measured NRM can be estimated, from which the "cleaned NRM" that represents the uncontaminated *in situ* remanence of the sample can be calculated.

For the scenario shown in Figure 4, the cleaned NRM directions of multiple samples will be distributed along a great circle path between the stable TRM and the recent field direction. The uncleaned measured NRMs of a sample collection are scattered away from this trend due to the IRM contamination. Note that the vectors denoted "cleaned NRM1" and "cleaned NRM2" in Figure 4 serve as approximate estimates of the uncontaminated *in situ* NRM. The former is somewhat "undercleaned", the latter slightly "overcleaned". The uncertainty in identifying the cleaned NRM direction simply by inspection, without using the quantitative analyses of multicomponent remanence mentioned above, arises because of overlapped stability spectra for the IRM and the other components. This overlap also means that a portion of the *in situ* VRM has been demagnetized by the time the IRM has been eliminated. However, if IRM contamination is minor, the original intensity of the VRM can be approximately estimated by extrapolation back to "zero demagnetization" of the demagnetization curve (intensity of vector differences versus demagnetization step) from the corresponding linear portion of the vector demagnetization diagram. A similar procedure can be applied to estimate the original uncleaned TRM intensity.

Referring to Figure 4, the NRM can be decomposed into contributions from the three isolated components:

$$\mathbf{M}_{\mathrm{NRM}} = M_1\hat{\mathbf{v}}_1 + M_2\hat{\mathbf{v}}_2 + M_3\hat{\mathbf{v}}_3, \tag{13}$$

where the hats on the $\mathbf{v}_i$ (i = 1,2,3) denote unit vectors along each of the remanence component directions. Taking dot products of the NRM vector with each of these unit vectors we get three equations in the three unknowns M_i:

$$\begin{aligned}
\mathbf{M}_{\mathrm{NRM}}.\hat{\mathbf{v}}_1 &= M_1 + M_2(\hat{\mathbf{v}}_2.\hat{\mathbf{v}}_1) + M_3(\hat{\mathbf{v}}_3.\hat{\mathbf{v}}_1),\\
\mathbf{M}_{\mathrm{NRM}}.\hat{\mathbf{v}}_2 &= M_1(\hat{\mathbf{v}}_2.\hat{\mathbf{v}}_1) + M_2 + M_3(\hat{\mathbf{v}}_3.\hat{\mathbf{v}}_2),\\
\mathbf{M}_{\mathrm{NRM}}.\hat{\mathbf{v}}_3 &= M_1(\hat{\mathbf{v}}_3.\hat{\mathbf{v}}_1) + M_2(\hat{\mathbf{v}}_2.\hat{\mathbf{v}}_3) + M_3,
\end{aligned} \tag{14}$$

which can be solved for M_i (i = 1,2,3). The cleaned NRM, appropriate for modelling, is then

$$\mathbf{M}_{\mathrm{cleaned}} = M_2\hat{\mathbf{v}}_2 + M_3\hat{\mathbf{v}}_3. \tag{15}$$

If only two components are present, the analogous procedure is even simpler. On the other hand, even if more components are present in the NRM, this approach can be applied sequentially to partly demagnetized remanence vectors, provided the stability spectra of the softest and hardest components are not overlapped. For example, if the stable remanence comprises primary TRM that is partially overprinted by a secondary component associated with metamorphism, the measured remanence vectors after removal of the IRM, or IRM and VRM, can be decomposed into contributions from the primary and metamorphic overprint magnetizations.

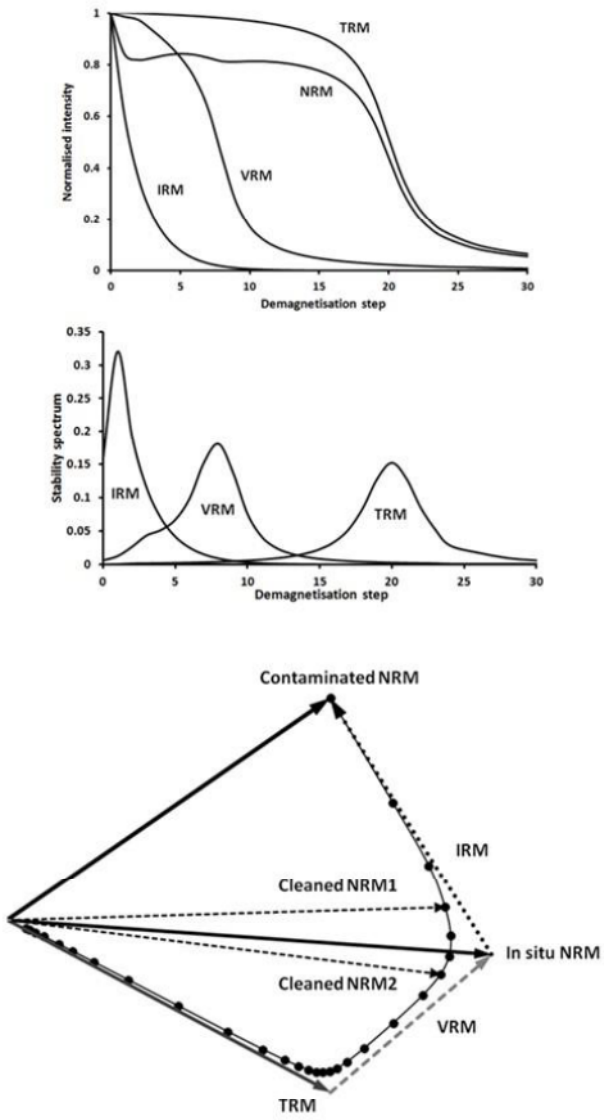

Figure 4. Palaeomagnetic cleaning of contaminated NRM to remove unrepresentative IRM noise and to estimate representative *in situ* remanence, which comprises a stable ancient TRM component and VRM acquired in the recent geomagnetic field (after Clark, 2014b).

It is clear from the discussion above that determination of representative bulk *in situ* remanence of a source from measurements on samples can be a non-trivial task, and that careful palaeomagnetic cleaning and analysis of demagnetization trends is essential if the NRM is multicomponent, or if significant contamination of measured NRMs occurs.

Clark and Tonkin (1994) present an example of a magnetic anomaly associated with strong, relatively complex, multicomponent remanent magnetization carried by pyrrhotitic metasediments in the Cobar area of New South Wales. Careful analysis of detailed AF and thermal demagnetization data on oriented drillhole samples enabled resolution of sample magnetizations into a normal component of moderate stability, overprinting a more stable component that could be of either polarity. Evaluating the average contributions of each component to the bulk

magnetization of the unit, and incorporation of drilling data that defined the geometry of the magnetic zone, enabled excellent quantitative agreement between the predicted and observed anomalies, confirming that the source had been intersected and the anomaly was predominantly associated with remanence. In simple cases, where measured NRMs have well-grouped directions that are clearly ancient and intensities are fairly consistent, analysis of NRM measurements is straightforward and very useful for constraining magnetic modelling.

Statistical analysis of multicomponent NRMs

The aim of the statistical analysis should be to calculate the population mean magnetization vector from a representative sample collection, because each approximately homogeneous small portion of a heterogeneous source contributes to the total magnetic moment in proportion to its magnetization times its volume. This means that, at distances that are large compared to the scale of heterogeneity, the magnetic anomaly is proportional to the arithmetic mean magnetization *vector*. Figure 5 shows how a mean remanence vector is calculated from sample remanence vectors. The mean total magnetization vector is calculated similarly.

However no rigorous methods have yet been developed for statistical estimation of error bounds on mean magnetization vectors when intensities and directions are both variable. A nonparametric method, such as bootstrapping, would probably be most suitable for this purpose.

A practical, albeit not rigorous, alternative to evaluate uncertainties in estimated magnetization vectors is to consider corresponding isolated components from the sample collection in turn. All the primary TRM components with the same polarity, for example, should be well grouped. If both polarities are present, each polarity subpopulation should be considered separately. The inferred TRM vector from each sample should be projected onto the vector mean TRM for the rock unit, yielding projected components that can be treated as a scalar variable. The sample standard deviation and confidence limits can be calculated from these data, using standard methods. Finally, reconstructed *in situ* NRM vectors can be calculated by summing the estimated remanence components and the effects of varying each component within its error bounds can be assessed.

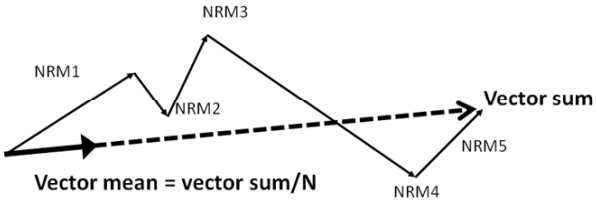

Figure 5. Calculation of vector mean NRM from measurements on five samples. The dashed line indicates the vector sum; the thick solid arrow represents the vector mean, calculated as the vector sum divided by the number of samples.

Statistical analysis of anisotropic susceptibility

If a sampled rock unit has anisotropic susceptibility, the induced magnetization of the unit should be estimated from the sample mean susceptibility tensor, obtained by summing the tensor components of all samples (with respect to a common reference frame) and dividing by the number of samples:

$$\overline{\mathbf{K}} = \frac{1}{n}\sum_{i=1}^{n}\mathbf{K}_i, \tag{16}$$

where the $\mathbf{K}_i$ are the susceptibility tensors for the individual samples. Parametric statistical methods have been developed for analyzing susceptibility anisotropy data in terms of average foliation planes and lineation directions. Constable and Tauxe (1990) developed a superior (albeit more complicated) nonparametric statistical method, using boot-strapping for estimating magnetic fabrics with confidence limits. As for estimation of error bounds on mean NRMs, a nonparametric method, such as boot-strapping, would probably be most suitable for statistical estimation of error bounds on mean susceptibility tensor data, when bulk susceptibilities and susceptibility ellipsoid shapes and orientations are all variable. For modelling purposes the most appropriate method is to calculate induced magnetization vectors from the sample susceptibility tensors and to analyse these as described above for remanence components.

Frequency-dependent susceptibility

Susceptibility measurements aimed at assisting magnetic modelling should be made at low frequencies (≤ 1 kHz) to minimize the effects of frequency dependent susceptibility and to ensure that measured susceptibility measurements are not unduly affected by high sample conductivity of, for example, massive sulfide ores (Worm et al., 1993; Yang and Emerson, 1997).

Measuring susceptibilities of samples at more than one frequency can be useful for characterizing the magnetic minerals present in a sample (Dearing, 1999). In particular a strong frequency dependence of susceptibility (> 2% decrease of susceptibility over a decade of frequency) of soil or rock samples indicates the presence of extremely fine-grained superparamagnetic particles in the sample. Complex AC susceptibility (with real and imaginary components) associated with superparamagnetism is characteristic of rocks and soils with strong frequency dependence of susceptibility and can produce observable effects in EM surveys (Buselli, 1982; Mutton, 2012; Gaucher and Smith, 2017).

Field-dependent susceptibility

Ideally, susceptibility instruments should operate at field strengths comparable to the geomagnetic field in order to minimise nonlinearity effects, which are important for multidomain (MD) pyrrhotite grains larger than about 30 µm (Clark, 1984; Worm et al., 1993; Martín-Hernández et al., 2008), for some high-Ti titanomagnetite-bearing rocks (Jackson et al., 1998), and for large MD hematite crystals (Guerrero-Suarez and Martín-Hernández, 2012).

When a weak magnetic field (one that is small compared to the coercive field H_c) is applied to an initially demagnetized material, the magnetization M_i of the

material often exhibits a quadratic dependence on the applied field H:

$$M_i(H) = \chi H + \eta H^2, \quad (H << H_c) \tag{17}$$

where χ is the initial susceptibility and η is the Rayleigh parameter. If the applied field cycles between values $\pm H_m$, the magnetization-field plot describes two parabolic arcs that together comprise a hysteresis loop, known as a Rayleigh loop (Figure 6). The IRM obtained after applying a field H_m to an initially demagnetized sample and then reducing the field to zero is given by

$$M_{IRM} = \frac{1}{2}\eta H_m^2. \tag{18}$$

Clark (2016) gives a comprehensive account of field-dependent susceptibility and implications for magnetic modelling and characterization of magnetic mineralogy.

Correcting measured magnetic properties for self-demagnetization

Hand-held susceptibility meters are calibrated for measurements on flat slabs and are best suited for measurements made on smooth, flat, fresh outcrops. For the commonly used hand-held meters calibration standards in the form of blocks or cakes with diameter ≥ 30 cm and thickness ≥ 15 cm are equivalent to infinite slabs. The fall-off with distance from the surface of the sample can be determined empirically using nonmagnetic spacers and used to make approximate corrections for outcrops with pronounced rugosity or a weathered crust. Use of these meters on drill core samples, split cores, small blocks etc. requires empirically determined correction factors that take the core diameter or block size into account (Schmidt and Lackie, 2014).

Hand-held susceptibility meter measurements made on strongly magnetic materials are affected by self-demagnetization. The meter produces a primary field, which induces a magnetization distribution in the sample. The meter detects the secondary field arising from this magnetization distribution. For a homogeneous magnetic half-space of susceptibility k, the boundary conditions for **B** and **H** at the rock-air interface imply that the secondary field above the half-space is everywhere proportional to $k/(1+k/2)$. This result can be obtained using the method of images. Provided that the susceptibility output of the meter is proportional to this secondary field, it follows that the apparent susceptibility k' of the half-space measured by the instrument is:

$$k' = k/(1 + k/2). \tag{19}$$

Equation (19) implies that the effective SI demagnetising factor at the interface for a homogeneous half-space is ½. The true susceptibility, found by inverting equation (9), is therefore:

$$k = k'/(1 - k'/2) \quad \text{[hand-held meter, large flat slab]}. \tag{20}$$

For strongly magnetic rocks, equation (20) should be used to correct the apparent susceptibilities given by hand-held susceptibility meters, assuming the output of the instrument

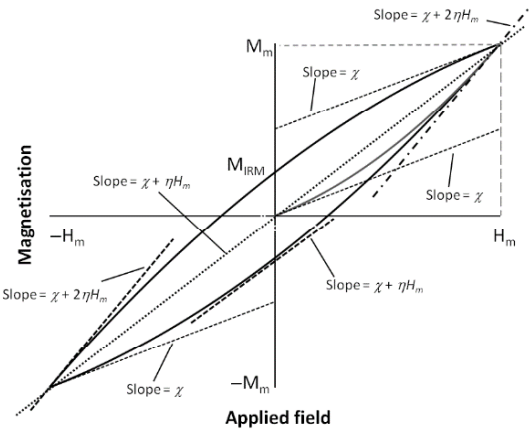

Figure 6. Intrinsic initial magnetization curve (solid grey line) and Rayleigh hysteresis loop (black) for a magnetic material with initial susceptibility χ and Rayleigh parameter η, for the case where $\chi = \eta H_{max}$. Note that the total differential susceptibility at each turning point of the loop, immediately after a field reversal, is equal to the initial susceptibility. The total differential susceptibility at all other points of the loop and along the initial magnetization curve, and the average susceptibility over the interval $[0,H_m]$ of the initial magnetization curve, are greater than χ.

is linear in the induced secondary field. It should be checked with the manufacturer whether or not the inherent nonlinearity described by equation (20) has been incorporated into the displayed output.

Equation (5) implies that both susceptibility and remanence measurements on strongly magnetic specimens need to be corrected for self-demagnetization, in order to obtain the intrinsic properties of the sampled material. The effect on susceptibility is dependent on the geometry of the sample/measuring instrument system, not just the sample shape. For isotropic susceptibility and equidimensional specimens, the intrinsic susceptibility of the specimen is given by:

$$k = k'/(1 - k'N_1), \tag{21}$$

and the intrinsic remanence is given by:

$$\mathbf{M}_{NRM} = (1 + kN_2)\,\mathbf{M}'_{NRM}, \tag{22}$$

where k is the intrinsic susceptibility, k' is the apparent susceptibility as measured by the instrument, N_1 is the demagnetising factor for the susceptibility instrument/sample configuration, $\mathbf{M}_{NRM}$ is the true remanence, $\mathbf{M}'_{NRM}$ is the apparent remanence and N_2 is the isotropic demagnetising factor of the isolated specimen. In the most general case, for inequidimensional, anisotropic specimens, the generalisations of (21) and (22) that yield demagnetization-corrected intrinsic properties are given by equation (5).

Analysis of the reluctance of the magnetic circuit for a ferromagnetic-cored transformer bridge shows that the SI demagnetising factor N_1 is approximately equal to the total

residual gap between the specimen and the poles of the magnetic core, divided by the total gap length. Therefore, if the specimen fills the entire gap, the demagnetising factor is effectively zero (neglecting leakage flux) and if the specimen is a very thin disc the demagnetising factor approaches its maximum value of 1.

For standard palaeomagnetic specimens, which have an isotropic demagnetization tensor, the SI demagnetising factor N_2 is 1/3, so

$$\mathbf{M}_{NRM} = \mathbf{M}'_{NRM}(1 + k/3), \tag{23}$$

where k is determined from (21).

If the field-dependence of susceptibility is significant, the initial magnetization curve of a strongly magnetic sample, subject to self-demagnetization, conforms to Rayleigh's laws, to a good approximation (provided the maximum applied field is not too strong):

$$M_i(H) \approx \chi' H + \eta' H^2, \quad (0 \le H \le H_m;\ \eta H_m << \chi) \tag{24}$$

where χ' and η' are the apparent or effective (demagnetization-limited) initial susceptibility and Rayleigh coefficient, given by

$$\chi' = \frac{\chi}{(1+N\chi)} \le \frac{1}{N}, \quad \eta' = \frac{\eta}{(1+N\chi)^3} = \frac{\eta}{(\chi/\chi')^3}. \tag{25}$$

Note that $\chi' < \chi$ and $\eta' < \eta$. The relations (19)-(25) are applicable to measurements made on a macroscopic homogeneous sample, or to the magnetization of a mineral grain in a rock, soil or ore. For magnetic materials with high intrinsic susceptibility, equation (25) implies, firstly, the well-known suppression of the apparent susceptibility by self-demagnetization and, secondly, an even stronger suppression of the Rayleigh coefficient. The shielding factor for the Rayleigh coefficient is equal to the cube of the shielding factor for the intrinsic susceptibility.

The intrinsic field-dependent susceptibility parameters can be determined from measured properties of a sample that is subject to self-demagnetization by inverting (25):

$$\chi = \frac{\chi'}{(1-N\chi')}, \tag{26}$$

$$\eta = \eta'(1+N\chi)^3 = \frac{\eta'}{(1-N\chi')^3} \quad (\eta H_m << \chi). \tag{27}$$

BOREHOLE LOGGING

The susceptibility of a source can be measured *in situ* by a borehole logging tool, or on samples extracted from the hole. If the hole intersects the source, a triaxial vector magnetometer with its orientation monitored continuously can measure the anomalous magnetic field within the source. Levanto (1963) and Bosum et al. (1988) describe orientation methods, presentation of data, and data analysis for borehole vector field measurements. For a uniformly magnetized source the anomalous internal **H** field of the source is:

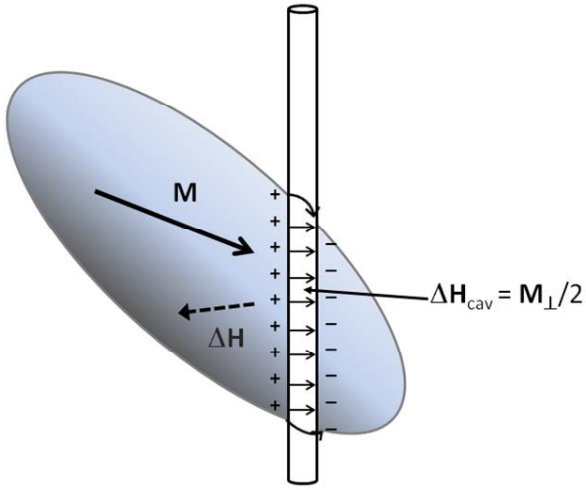

Figure 7. Relationship between internal anomalous field within a magnetized body, given by equation (28), and the field within the borehole.

$$\Delta\mathbf{H} = -\mathbf{N}\mathbf{M}, \tag{28}$$

where **N** is the demagnetizing tensor determined by the shape of the source.

For ellipsoidal bodies, including limiting cases such as spheres, infinite circular and elliptic cylinders, and infinite sheets, **N** is uniform throughout the body (Clark et al., 1986). In the interior of uniformly magnetized non-ellipsoidal bodies, **N** is a slowly varying function of position within the body.

As shown in Figure 3, a magnetometer in a borehole does not measure the anomalous field $\Delta\mathbf{B} = \mu_0\Delta\mathbf{H}$, where $\Delta\mathbf{H}$ is the self-demagnetizing field, given by (28). Instead it measures the field within the cylindrical borehole cavity, $\Delta\mathbf{B}' = \mu_0\Delta\mathbf{H}'$, which has components parallel to (||) and perpendicular to (⊥) the borehole that are given by

$$\Delta B_{\parallel}' = \mu_0 \Delta H_{\parallel}, \quad \Delta\mathbf{B}_{\perp}' = \mu_0[\Delta\mathbf{H}_{\perp} + \mathbf{M}_{\perp}/(\mu_r+1)], \tag{29}$$

where $\mu_r = 1+\chi$ is the relative permeability.

For the important case of a layer cake stratigraphy, the demagnetizing factors of a horizontal sheet are $N_{x,y} = 0$, $N_z = 1$. Figure 8 shows the relationships between the borehole field, the external field, and the bulk internal field away from the borehole, for a vertical hole through a thick horizontal layer. For most rock units $\chi << 1$, in which case $\mu_r + 1 = 2+\chi \approx 2$. In this approximation, the magnetization of the sheet can be inferred directly from the step change in measured magnetic field components within the borehole as it crosses into or out of the sheet, without measuring the susceptibility. For strongly magnetic layers however, the susceptibilities need to be known in order to calculate the magnetization exactly.

If a vertical borehole crosses the interface between two horizontal layers with susceptibilities χ_1 and χ_2 and magnetizations $\mathbf{M}_1$ and $\mathbf{M}_2$ respectively, the magnetization contrast $\Delta\mathbf{M} = \mathbf{M}_2 - \mathbf{M}_1$ between the layers is given by:

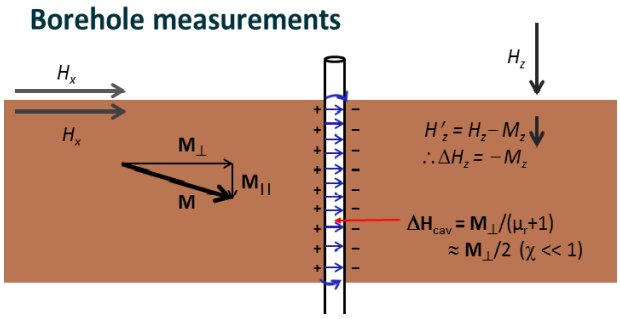

Figure 8. Determination of magnetization vector for a thick homogeneously magnetized layer, using borehole vector magnetometry. The external anomalous field is zero. Within the layer the internal anomalous field is uniform and is antiparallel to the magnetization component that is perpendicular to the plane of the magnetized sheet.

$$\Delta M_z = -\Delta B_z / \mu_0,$$
$$\Delta M_{x,y} = \frac{(B_{x,y})_2/\mu_0}{2+\chi_2} - \frac{(B_{x,y})_1/\mu_0}{2+\chi_1} \approx 2\Delta B_{x,y}/\mu_0. \quad (30)$$

The absolute magnetizations can be determined by tracking the magnetization contrasts back to a nonmagnetic layer or to the surface. These relationships can be easily generalized to the case of a nonvertical borehole or to dipping beds, provided the dip is known.

Equation (30) is valid for a smooth-walled borehole within the body, when measurements are taken at least several borehole diameters beneath its upper boundary, or above its lower boundary, *provided the magnetization is uniform over several borehole diameters around the measurement point*. Close to the boundary more complicated equations given by Pozzi et al. (1988) or Gallet and Courtillot (1989) can be used. If the geometry of the source is known or assumed, **N** is specified and the magnetization can then be deduced from equations (28) and (30).

In practice small scale heterogeneity adjacent to the borehole and rugosity of its wall often make vector measurements inside a strongly magnetic source quite noisy. However these local perturbations average to zero over larger distances, so the bulk magnetization of the source can be estimated reasonably accurately by averaging measured vectors throughout the borehole intersection. The major source of noise in downhole vector measurements is misorientation of the magnetometer. Orientation errors of ~0.1° produce errors of several tens of nT in vector components, which translate to errors in estimated magnetization components of ~10-100 mA/m.

ANALYSIS OF MAGNETIC ANOMALIES

Determination of magnetization direction from analysis of magnetic anomalies has a long history, dating back at least to Hall (1959). Modelling of magnetic anomalies without independent geological information can be ambiguous. For example, the magnetization direction of a semi-infinite dipping sheet cannot be uniquely determined from its anomaly, unless the dip is known (see Figure 9). If the

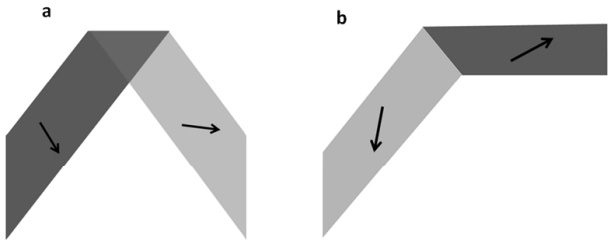

Figure 9. Strictly equivalent 2D sources: (a) equivalent dipping sheets, (b) equivalent sloping step and dipping sheet. The dipping sheets have infinite depth extent, the sloping step extends to infinity towards the RHS. Radhakrishna Murthy (1985) showed that any two dipping sheets, with differing magnetizations, that form an anticline are equivalent to a step whose sloping face coincides with the axial plane of the anticline.

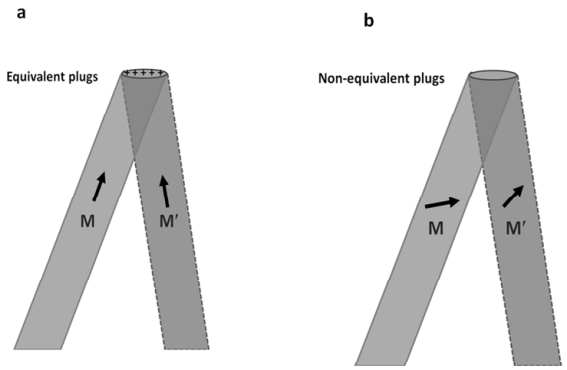

Figure 10. (a) Equivalent plunging pipes of infinite depth extent with axial magnetization, (b) non-equivalent pipes with non-axial magnetizations. For case (a) the anomaly arises purely from the poles induced on the top surface of the pipes. Since both pipes produce an identical pole distribution, their anomalies are identical. When there is a non-axial component of magnetization, as shown in (b), the poles induced on the flanks of the pipes ensure that pipes with different plunges produce different anomaly patterns over the measurement plane.

sheet also produces a well-defined gravity anomaly, however, the dip is constrained and the ambiguity is resolved. In this case the magnetization direction within the plane normal to strike can be determined by applying Poisson's theorem. Of course, any other method that determines the dip, such as drill hole intersections or seismic data, also suffices to determine the effective magnetization in the plane perpendicular to strike, $\mathbf{M}_\perp$.

Inversion of potential field data, including magnetic, is fundamentally non-unique (see Clark (2014b) for a review). There are many circumstances, however, in which the inherent non-uniqueness of magnetic inversion is not as serious a problem as is commonly suggested, as some important information can be extracted without any *a priori* information and even minimal additional information can greatly constrain acceptable models (Saltus and Blakely, 2011).

For isolated compact sources, the magnetic moment and direction of magnetization (3D case), or the magnetic moment per unit length and magnetization direction projected onto the plane normal to strike (2D case), can be modelled accurately without any knowledge of the size and shape of the source. On the other hand, if the geometry of an arbitrary homogeneous source is known (e.g. defined by drilling or other geophysical methods) determination of the magnetization of the source from the observed anomaly is a straightforward linear inversion problem (Bott, 1973; Blakely, 1996, p.225-228).

In general, even if the geometry of a 3D source is not known accurately, inferring its magnetization direction from the anomaly is inherently less ambiguous than for a 2D source. Figure 10 illustrates this for a plunging pipe, where the magnetization direction and plunge of the pipe can be estimated independently provided there is a transverse component of magnetization. This is so, even though this source does not meet the criterion of compactness.

Clark (2014b) gives a comprehensive review of methods of determining magnetization of sources from analysis of their magnetic anomalies. These methods include:

- constrained modelling/inversion of anomalies,
- direct simple inversions of measured or calculated vector and gradient tensor data for simple sources,
- retrospective inference of magnetization of a mined deposit by comparing magnetic data acquired pre- and post-mining,
- combined analysis of magnetic and gravity anomalies using Poisson's theorem,
- Helbig-type analysis, based on integral moments of gridded vector components, gradient tensor elements, and tensor invariants, evaluated over the full extent of an isolated anomaly,
- methods based on reduction to the pole and related transforms,
- remote *in situ* determination of NRM direction, total magnetization direction and Koenigsberger ratio by deploying dual vector magnetometers or a single combined gradiometer/magnetometer to monitor local perturbation of natural geomagnetic variations, operating in base station mode within a magnetic anomaly of interest.

Clark (2014b) also discusses some other methods for obtaining information about magnetization of sources, apart from those mentioned above, including:

- using a controlled magnetic source to probe the susceptibility distribution of the subsurface,
- inference of properties from petrographic/ petrological information, supplemented by palaeomagnetic databases.

Table 1 summarizes the assumptions that underlie each of these methods, the information about magnetization that each provides, and the limitations of each method.

CONCLUSIONS

Information about magnetization of sources is essential for reliable interpretation of magnetic survey data and for constraining modelling of magnetic sources. A number of approaches are available to determine the contributions of induced and remanent magnetization to the observed magnetic anomalies. An understanding of the geological controls on magnetization can inform interpretation of magnetic data in geological terms. Petrophysical measurements on outcrop and drill core samples provide useful "ground truth" for constraining interpretation, but sampling, measurement protocols and statistical analysis must be performed correctly to obtain maximum benefit. Magnetic petrological principles can help to guide interpretations. Borehole magnetic measurements can provide valuable information on magnetic properties of intersected rock formations. In many cases careful analysis of individual magnetic anomalies, particularly in conjunction with other geological or geophysical information, can accurately estimate source magnetization directions, thereby constraining modelling and providing useful geological information about the geological history of the study area.

REFERENCES

Aitchison J., 1955, On the distribution of a positive random variable having a discrete probability mass at the origin: Journal of the American Statistical Association, 50(271), 901-908.

Aitchison, J. and Brown, J.A., 1963, The Lognormal Distribution with Special Reference to its Use in Economics, Cambridge University Press.

Blakely, R.J., 1996, Potential Theory in Gravity and Magnetic Applications, Cambridge University Press.

Bosum, W., Eberle, D., and Rehli, H.J., 1988, A gyro-oriented 3-component borehole magnetometer for mineral prospecting, with examples of its application: Geophysical Prospecting, 36(8), 933-961.

Bott, M.H.P., 1973, Inverse methods in the interpretation of magnetic and gravity anomalies, in Bruce A. Bolt, ed., Methods in Computational Physics: Advances in Research and Applications, 13, 133-162, Elsevier.

Buselli, G., 1982, The effect of near-surface super-paramagnetic material on electromagnetic measurements: Geophysics, 47, 1315-1324.

Clark, D.A., 1984, Hysteresis properties of sized dispersed monoclinic pyrrhotite grains: Geophysical Research Letters, 11, 173-176.

Clark, D.A., 1997. Magnetic petrophysics and magnetic petrology: aids to geological interpretation of magnetic surveys. AGSO Journal of Australian Geology and Geophysics, 17, 83-103.

Clark, D.A., 1999, Magnetic petrology of igneous intrusions: implications for exploration and magnetic interpretation. Exploration Geophysics, 30, 5-26.

Clark, D.A., 2014a. Magnetic effects of hydrothermal alteration in porphyry copper and iron-oxide copper–gold systems: A review, Tectonophysics, 624-625, 46-65. http://dx.doi.org/10.1016/j.tecto.2013.12.011

Clark, D.A., 2014b, Methods for determining remanent and total magnetisations of magnetic sources - a review: Exploration Geophysics, 45, 271–304. http://dx.doi.org/10.1071/EG14013.

Clark, D.A., 2016. Field-dependent susceptibility of rocks and ores – implications for magnetic petrophysics and magnetic modelling: ASEG Extended Abstracts, ASEG-PESA-AIG Conference, August 21-24, 2016, Adelaide, Australia, 926-934.

Clark, D. A. and Tonkin, C., 1994. Magnetic anomalies due to pyrrhotite: examples from the Cobar area, N.S.W., Australia: Journal of Applied Geophysics, 32, 11-32.

Clark, D.A., Saul, S.J. and Emerson, D.W., 1986, Magnetic and gravity anomalies of a triaxial ellipsoid: Exploration Geophysics, 17, 189-200.

Constable, C. and Tauxe, L., 1990, The bootstrap for magnetic susceptibility tensors: Journal of Geophysical Research, 95(B6), 8383–8395,

Dearing, 1999. Environmental magnetic susceptibility using the Bartington *MS2* system. http://gmw.com/magnetic_properties/pdf/Om0409%20J_Dearing_Handbook_iss7.pdf, accessed August 10, 2017.

Emerson, D.W., Clark, D.A. and Saul, S.J., 1985, Magnetic exploration models incorporating remanence, demagnetisation and anisotropy: HP 41C handheld computer algorithms: Exploration Geophysics, 16, 1-122.

Gallet, Y. and Courtillot, V., 1989, Modeling magnetostratigraphy in a borehole: Geophysics, 54(8), 973-983.

Gaucher, F.E. and Smith, R.S., 2017, The impact of magnetic viscosity on time-domain electromagnetic data from iron oxide minerals embedded in rocks at Opemiska, Québec, Canada: Geophysics, 82(5), B165-B176.

Guerrero-Suarez, S., and Martin-Hernandez, F., 2012, Magnetic anisotropy of hematite natural crystals: increasing low-field strength experiments: International Journal of Earth Sciences, 101, 625-636.

Hall, D.H., 1959, Direction of polarization determined from magnetic anomalies: Journal of Geophysical Research, 64, 1945-1959.

Halls, H. C., 1976. A least-squares method to find a remanence direction from converging remagnetization circles. Geophysical Journal of the Royal Astronomical Society, 45: 297–304.

Halls, H.C., 1979. Separation of multicomponent NRM: combined use of difference and resultant magnetization vectors, Earth and Planetary Science Letters, Volume 43, 303-308.

Hoffman, K. A. and Day, R., 1978, Separation of multicomponent NRM: A general method: Earth and Planetary Science Letters, 40, 433–438.

Jackson, M., Moskowitz, B., Rosenbaum, J. and Kissel, C., 1998, Field-dependence of AC susceptibility in titanomagnetites: Earth and Planetary Science Letters, 157, 129-139.

Kent, J. T., Briden, J. C. and Mardia, K. V., 1983, Linear and planar structure in ordered multivariate data as applied to progressive demagnetization of palaeomagnetic remanence: Geophysical Journal of the Royal Astronomical Society, 75(3), 593-621.

Kirschvink, J. L., 1980, The least-squares line and plane and the analysis of palaeomagnetic data: Geophysical Journal of the Royal Astronomical Society, 62, 699–718.

Levanto, A.E., 1963, On magnetic measurements in drill holes: Geoexploration, 1(2), 8-20.

Martin-Hernandez. F, Dekkers, M.J., Bominaar-Silkens, I.M.A., and Maan, J.C., 2008, Magnetic anisotropy behaviour of pyrrhotite as determined by low- and high-field experiments: Geophysical Journal International, 174, 42-54.

McFadden, P.L. and McElhinny, M.W., 1988, The combined analysis of remagnetization circles and direct observations in palaeomagnetism: Earth and Planetary Science Letters, 87, 161-172.

Mutton P., 2012, Superparamagnetic effects in EM surveys for mineral exploration, in ASEG Extended Abstracts 2012, Australian Society of Exploration Geophysicists.

Owen, W.J. and DeRouen, T.A., 1980. Estimation of the mean for lognormal data containing zeroes and left-censored values, with applications to the measurement of worker exposure to air contaminants: Biometrics, 36(4), 707-719.

Pozzi, J. P., Martin, J. P., Pocachard, J., Feinberg, H., and Galdeano, A., 1988, In-situ magnetostratigraphy: interpretation of magnetic logging in sediments: Earth and Planetary Science Letters, 88, 357-373.

Puranen, R., 1989, Susceptibilities, iron and magnetite content of Precambrian rocks from Finland: Geological Survey of Finland Report of Investigations, 90, 45 pp.

Saltus, R.W. and Blakely, R.J., 2011, Unique geologic insights from "non-unique" gravity and magnetic interpretation: GSA Today, 21(12), 4-11.

Radhakrishna Murthy, I.V., 1985, Magnetic equivalence of dipping beds, faults and anticlines: Pure and Applied Geophysics, 123, 893-901.

Schmidt, P. W., 1982. Linearity spectrum analysis of multi-component magnetizations and its application to some igneous rocks from south-eastern Australia. Geophysical Journal of the Royal Astronomical Society, 70: 647–665.

Schmidt, P.W., 1985. Bias in converging great circle methods, Earth and Planetary Science Letters, 72, 427-432.

Schmidt, P.W. and Lackie, M.A., 2014, Practical considerations: making measurements of susceptibility, remanence and Q in the field: Exploration Geophysics, 45, 305-313.

Worm, H. U., Clark, D., and Dekkers, M. J., 1993, Magnetic susceptibility of pyrrhotite: grain size, field and frequency dependence: Geophysical Journal International, 114, 127-137.

Yang, Y. P. and Emerson, D. W., 1997, Electromagnetic conductivities of rock cores: theory and analog results: Geophysics, 62(6), 1779-1793.

Table 1. Comparison of different methods for determination of source magnetization

METHOD	ASSUMPTIONS/RESTRICTIONS/ REQUIREMENTS	PARAMETERS ESTIMATED	LIMITATIONS
Sample measurements	• Representative sampling • Sufficient sampling • NRM uncontaminated or cleanable • Adequate statistical analysis and appropriate treatment of vectors	k or $\mathbf{K}$, $\mathbf{M}_{IND}$, $\mathbf{M}_{NRM}$, $\mathbf{M}$, Q	• Unavailability of samples • Available samples unrepresentative • Remanence contaminated • Weathering • Heterogeneity, nugget effect • Requires sophisticated equipment for complex NRM
Borehole measurements (vector magnetometer + susceptibility logging)	• Uniform properties within intersected source • Layered earth with known dips, or known shape of intersected source • Hole intersects source(s)	k, $\mathbf{M}_{IND}$, $\mathbf{M}_{NRM}$, $\mathbf{M}$, Q	• Source geometry may be unknown (possibly can be modelled by external measurements) • Orientation noise on vector measurements • Noisy vectors due to heterogeneity and rugosity
Petrology + palaeopole database	• Good petrographic descriptions • Known geological history • Events with well-defined ages or plausible age range	k, $\mathbf{M}_{IND}$, $\sim\lvert\mathbf{M}_{NRM}\rvert$, $\sim\mathbf{M}$, $\sim Q$	• Petrological information may be insufficient • Complex history • Age uncertainty • APWP poorly known • Unknown local tectonic rotations
Constrained modelling/inversion	• Source assumed to be non-pathological • Magnetic data only: unique inversion of geometry requires assuming homogeneity, planar faces, single intersection with every vertical line through body, noise-free data • Magnetics + geometry from other methods: requires assuming homogeneity	*Compact 2D source*: $\mathbf{M}_\perp A$, $\mathbf{M}_\perp / \lvert\mathbf{M}_\perp\rvert$ *Compact 3D source*: $\mathbf{m} = \mathbf{M}V$, $\mathbf{M}/\lvert\mathbf{M}\rvert$ *2D finite equivalent sources*: $\mathbf{M}_\perp A$, $\mathbf{M}_\perp / \lvert\mathbf{M}_\perp\rvert$ *3D finite equivalent sources*: $\mathbf{m} = \mathbf{M}V$, $\mathbf{M}/\lvert\mathbf{M}\rvert$ *Unique 2D polygon*: $\mathbf{M}_\perp$ *Unique 3D polyhedron*: $\mathbf{M}$ *Defined 2D geometry*: $\mathbf{M}_\perp$ *Defined 3D geometry*: $\mathbf{M}$	• Geometry can be non-unique if unconstrained, implying magnetization intensity is indeterminate and direction may be inaccurate • Uniqueness requires special assumptions or extra information • Sensitive to noise, unremoved regional trends, under-sampling etc.

Table 1 (continued). Comparison of different methods for determination of source magnetization

Simple direct inversions for simple sources	• Source type must be assumed or constrained, e.g. dipole model: compact 3D source/homogeneous sphere/equidimensional source not too close to sensor • Source location must be inverted first	$\mathbf{m} = \mathbf{M}V$, $\mathbf{M}/\lvert\mathbf{M}\rvert$ (dipole) $\mathbf{M}A$, $\mathbf{M}/\lvert\mathbf{M}\rvert$ (narrow vertical pipe) $\mathbf{M}_\perp A$, $\mathbf{M}_\perp/\lvert\mathbf{M}_\perp\rvert$ (2D horizontal cylinder) $\mathbf{M}_\perp t$, $\mathbf{M}_\perp/\lvert\mathbf{M}_\perp\rvert$ (2D thin sheet) $\mathbf{M}_\perp$, $\mathbf{M}_\perp/\lvert\mathbf{M}_\perp\rvert$ (2D thick sheet/contact)	• Source may not conform to assumed form • Requires vector or gradient tensor data to be measured or to be accurately calculable from sufficiently high quality TMI data
Comparison of magnetic surveys before and after removal of source	• Known geometry of removed material (to determine $\overline{\mathbf{M}}$) • Homogeneous magnetization (to determine **M**)	$\mathbf{m} = \mathbf{M}V$; $\overline{\mathbf{M}}$, **M**, $\mathbf{M}_{IND}$, $\mathbf{M}_{NRM}$, **M**, Q (if k of removed material has been measured	• Requires high quality magnetic surveys both before and after removal of source • Requires 3D delineation of source
Combined magnetics and gravity (based on Poisson's relation)	• Assumes common source for magnetic and gravity anomalies (shape does not need to be known) • Assumes homogeneous density and magnetization, or at least constant $\lvert\mathbf{M}\rvert/\rho$ and constant direction of **M**	$\lvert\mathbf{M}\rvert/\rho$, $\mathbf{M}/\lvert\mathbf{M}\rvert$,	• Sources of gravity and magnetic anomalies are often not identical • Density or magnetization contrast may be insufficient to generate anomaly that can be accurately separated from background trends and noise
Active source magnetics	• Roving primary source field is accurately known across survey area • Measurements are made sufficiently long after switching primary field that eddy currents in subsurface have decayed • For frequency domain methods: f is low enough to provide required penetration depth; subsurface is (i) homogeneous half-space, or (ii) 1D, over footprint of system	k, $\mathbf{M}_{IND}$	• Rapid fall-off restricts method to shallow sources, with tradeoff between depth of penetration and spatial resolution of subsurface magnetization distribution • Complex geology/dipping interfaces/high conductivities can make apparent susceptibilities inaccurate • Does not detect remanence

Table 1 (continued). Comparison of different methods for determination of source magnetization

Helbig-type analysis	• Source has limited lateral and depth extents (geometry otherwise arbitrary) and is well separated from neighbouring sources • Magnetic data are sufficiently high quality to define vector and/or tensor components accurately over extensive area	$\mathbf{m} = \mathbf{M}V$, $\mathbf{M}/\lvert\mathbf{M}\rvert$	• Source may extend beyond survey area, or have large depth extent • Interference from neighbouring anomalies • Unremoved regional trends • Requires depth of centroid estimate for accurate calculation of moment magnitude, corrected for finite range of integration
Methods based on RTP and other transforms	• Stable algorithm for RTP and other transforms, such as pseudogravity • Assumes constant direction of magnetization throughout source • Works best for compact sources, steeply dipping tabular bodies, steeply plunging pipes and steep contacts	$\mathbf{M}/\lvert\mathbf{M}\rvert$	• Instability of RTP at low latitudes • Sources may have shallow dipping sides • Interference from neighbouring anomalies with different directions of **M**
Base station DVM/magnetometry-gradiometry	• Assumes homogeneous source • Assumes induced magnetization is parallel to inducing field (deflection due anisotropy or self-demagnetization requires multiple stations)	*Compact 2D source*: $\mathbf{M}_\perp A$, $\mathbf{M}_\perp/\lvert\mathbf{M}_\perp\rvert$, $\mathbf{M}_\perp/k$, $(\mathbf{M}_\perp)_{NRM}/k$, $(\mathbf{M}_\perp)_{NRM}/\lvert(\mathbf{M}_\perp)_{NRM}\rvert$, Q, centroid *Compact 3D source*: $\mathbf{m} = \mathbf{M}V$, $\mathbf{M}/\lvert\mathbf{M}\rvert$, $\mathbf{M}/k$, $\mathbf{M}_{NRM}/k$, $\mathbf{M}_{NRM}/\lvert\mathbf{M}_{NRM}\rvert$, Q, centroid *Arbitrary 2D source*: $\mathbf{M}_\perp/k$, $\mathbf{M}_\perp/\lvert\mathbf{M}_\perp\rvert$, $(\mathbf{M}_\perp)_{NRM}/k$, $(\mathbf{M}_\perp)_{NRM}/\lvert(\mathbf{M}_\perp)_{NRM}\rvert$, Q, centroid *Arbitrary 3D source*: $\mathbf{M}/k$, $\mathbf{M}/\lvert\mathbf{M}\rvert$, $\mathbf{M}_{NRM}/k$, $\mathbf{M}_{NRM}/\lvert\mathbf{M}_{NRM}\rvert$, Q, centroid	• Non-compact source may be inhomogeneous • Induced magnetization may be deflected by strong anisotropy or self-demagnetization • Very high Q may make induced signal indeterminate and solution unobtainable • Requires very sensitive gradiometers, or very accurately aligned vector magnetometers